Available online at www.sciencedirect.com
ScienceDirect
Polymer 48 (2007) 5408–5416
polymer
www.elsevier.com/locate/polymer

Characterization, crystallization kinetics and melting behavior of poly(ethylene succinate) copolyester containing 5 mol% trimethylene succinate

Ming Chen*, Wei-Che Chang, Hsin-Ying Lu, Chi He Chen, Jyun-Siang Peng, Chia-Jung Tsai

Institute of Materials Science and Engineering, National Sun Yat-Sen University, 70 Lien Hai Road, Kaohsiung 80424, Taiwan, ROC

Received 29 January 2007; received in revised form 22 June 2007; accepted 27 June 2007
Available online 4 July 2007

Abstract

Copolyester was synthesized and characterized as having 94.4 mol% ethylene succinate units and 5.6 mol% trimethylene succinate units in a random sequence as revealed by NMR. Differential scanning calorimeter (DSC) was used to investigate the isothermal crystallization kinetics of this copolyester in the temperature range (T_c) from 30 to 80 °C. The melting behavior after isothermal crystallization was studied by using DSC and temperature modulated DSC (TMDSC) by varying the T_c, the heating rate and the crystallization time. DSC and TMDSC curves showed triple melting peaks. The melting behavior indicates that the upper melting peaks are primarily due to the melting of lamellar crystals with different stabilities. A small exothermic curve between the main melting peaks gives a direct evidence of recrystallization. As the T_c increases, the contribution of recrystallization gradually decreases and finally disappears. The Hoffman–Weeks linear plot gave an equilibrium melting temperature of 108.3 °C. The kinetic analysis of the spherulitic growth rates indicated that a regime II → III transition occurred at ~65 °C.

Keywords: Copolyester; Poly(ethylene succinate); Crystallization

1. Introduction

Polymers universally used such as polyethylene (PE), polypropylene (PP) and polystyrene have caused considerable environmental pollution since they are not degradable but stable. With the rise of concern to global environment in recent years, much attention has been focused on biodegradable and biocompatible polymers. According to the difference in the preparation methods, biodegradable polymers can be classified into two types. One is the biosynthetic polymer, such as bacterial polyhydroxyalkanoates (PHAs). The other is the chemosynthetic polymer, such as aliphatic polyesters. Aliphatic polyesters are considered to be biodegradable plastics owing to their susceptibilities to enzymes and microorganisms. Poly(ethylene succinate) (PES) has a comparatively high melting point (103–106 °C) [1] and some good mechanical properties, which are comparable with some of the extensively used polymers like low density PE (LDPE), PP, etc.

Among the properties of biodegradable polymeric materials, biodegradation rate is the most important for practical application. Numerous factors affect the biodegradation rates of polymers, such as chemical composition, crystalline structure, and morphology [2]. Many researchers have found that the degree of crystallinity, spherulite size and lamellar structure of the aliphatic polyesters can influence the biodegradation rate, because biodegradation first takes place at the amorphous parts of polymers [3]. Accordingly, crystallization kinetics and melting behaviors should be carefully considered, since they affect not only the crystallinity of polymers but also the final physical properties and biodegradability.

Poly(trimethylene succinate) (PTS) is a new polyester with an odd number of methylene groups in its respective diol monomer. Poly(butylene succinate) (PBS), PTS and PES are only different in their numbers of methylene groups between

* Corresponding author. Tel.: +886 7 382 4680; fax: +886 7 525 4099.
E-mail address: mingchen@mail.nsysu.edu.tw (M. Chen).

0032-3861/$ - see front matter © 2007 Published by Elsevier Ltd.
doi:10.1016/j.polymer.2007.06.060

the two ether groups, namely 4, 3 and 2, respectively. It was found that PTS which had the lowest crystallinity degraded faster than PBS and PES [4]. The crystal structure [5–8] and the crystal growth kinetics [2,9] of PES have been studied. The molecular weight dependence of the crystallization rate and the primary nucleation rate of PES have also been investigated [10,11]. Only a few studies on the multiple melting behavior of PES have been published [2,9,12–14].

Tsai et al. synthesized PES, PTS and a series of their copolymers [1]. They identified that the distribution of ethylene succinate (ES) and trimethylene succinate (TS) units in these copolyesters is random. Results of wide-angle X-ray diffraction (WAXD) and heating thermograms for the measurements of melting (T_m) and glass transition (T_g) temperatures indicate that the incorporation of TS units into PES significantly inhibits the crystallization behavior of PES. The crystallinity falls from 34 to 8% as the TS content increases from 0 to 50%. Additionally, the value of T_g decreases from −9.9 to −31.5 °C as TS increases from 0 to 100%. Therefore, in this study, PES copolymer with only 5 mol% TS was synthesized and characterized. To the best of our knowledge, poly[(ethylene succinate)-*co*-(5 mol% trimethylene succinate)] (PES-*co*-5%PTS) has not been reported so far in the literature. In this study, the differential scanning calorimetric (DSC) data were analyzed over a wide range of isothermal crystallization temperature (T_c) using the Avrami equation [15,16]. The origin of the multiple melting behavior of isothermal crystallized specimens was elucidated using WAXD, DSC and temperature modulated DSC (TMDSC) by varying the T_c, the crystallization time and the heating rate. The linear growth rates of spherulites were obtained using a polarized light microscope (PLM) and the regime transition temperature was determined from the Lauritzen–Hoffman (LH) equation [17].

2. Experimental

2.1. Synthesis and characterization

Ethylene glycol (EG) (Showa, 99.5%), 1,3-propanediol (PD) (Acros, 98%) and succinic acid (SA) (Acros, 99%) were used without purification. Titanium tetraisopropoxide (TTP) (Acros, 98+%) was used as received. Other solvents for analysis were also used without further purification. The reaction mixture was charged into a 1-L stainless reactor with the molar ratios of EG:PD:SA = 0.95:0.05:1. TTP was used as a catalyst with 0.1 mol% based on the amount of diacid used. PES-*co*-5%PTS copolyester was synthesized by a two-step esterification reaction in the melt. It was purified after dissolving in chloroform and precipitating into 10-fold amount of vigorously stirred ice-cooled methanol. The precipitate was filtered, washed with methanol, and dried under reduced pressure at room temperature.

This copolyester had an intrinsic viscosity [η] of 1.01 dL/g, measured in phenol/1,1,2,2-tetrachloroethane (3/2, w/w) at 30 °C. The number and weight average molecular weights, M_n and M_w, were 8.4×10^4 and 1.37×10^5 g/mol relative to poly(methyl methacrylate), respectively. A detailed report of characterization of a series of other PES/PTS random copolymers simply referred our most recent work [1]. The T_g of an amorphous specimen was obtained with a Perkin–Elmer Pyris 1 DSC at a heating rate of 10 °C/min. The corresponding T_g was −11.6 °C (261.5 K).

All the PES-*co*-5%PTS sheets were prepared in a hot press machine. The compressed sheet had a thickness of about 0.2 mm for DSC studies or about 0.5 mm for WAXD patterns. Both purified PES-*co*-5%PTS and sheets were dried at room temperature in a vacuum oven for 12 h to remove moisture before use.

2.2. ^{13}C NMR analysis

The NMR spectrum of $CDCl_3$ solution was recorded using a Varian UNITY INOVA-500 NMR spectrometer at 295.5 K. Fig. 1 presents the ^{13}C NMR spectrum of the copolymer and the peak assignments. The two chemical shifts at 61.19–62.34 and 28.73–28.90 ppm are associated with the methylene carbons α and β to the ester oxygen in the trimethylene group [1]. The diol carbon atoms of ethylene group are at 62.35 ppm (C_2). The chemical shifts of methylene group and the carbonyl group of succinic acid are at 27.80–27.84 (C_1) and 172.89–173.05 (C_5) ppm, respectively. In a closer view of the ^{13}C NMR spectrum, the carbonyl carbons (C_5) were split into three peaks, as shown in the inset of Fig. 1. The assigned b–d peaks represent the carbonyl carbons of EST-T side, EST-E side and ESE structures, respectively (where E represents EG unit, S represents SA unit, and T denotes PD unit).

A detailed determination of compositions and the ester sequence distribution of a series of other PES/PTS random copolymers were reported in our most recent work [1]. This copolyester is characterized as having 94.4% ES units and 5.6% TS units, based on the analysis of carbonyl carbons. ES and TS units had average-number sequence length of 16.8 and 1.0, respectively. The randomness, B, is 1.06, which is within experimental error, $B = 1.0$ for a random copolyester. Therefore, the distribution of ES and TS units in this

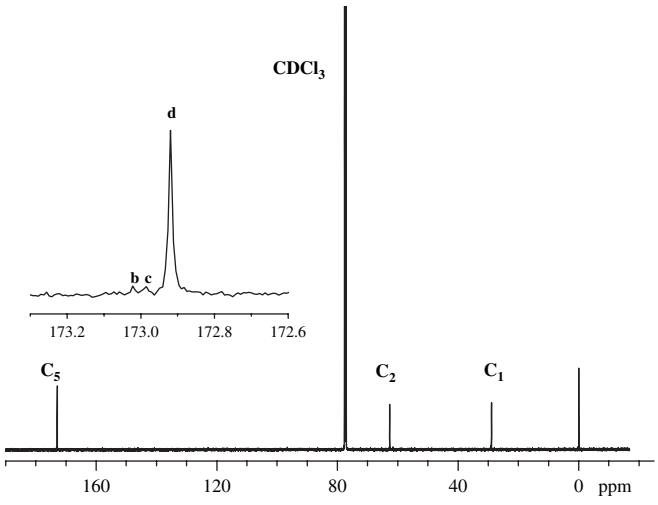

Fig. 1. ^{13}C NMR spectrum (solvent: $CDCl_3$ at 295.5 K) and its peak assignments.

copolyester is supposed to be random from the evidence of a single T_g at −11.6 °C and a randomness value of 1.06.

2.3. Differential scanning calorimetry (DSC) and specimens' preparation

A Perkin–Elmer Pyris 1 DSC, equipped with a refrigerating system (Pyris Intracooler 2P), was routinely calibrated with deionized water and indium. The heat of fusion was calibrated with indium. About 2–4 mg of sample was used. In the isothermal crystallization study, the samples were initially heated from 30 to 160 °C at 20 °C/min and then held in a molten state for 5 min. They were then quickly cooled at a nominal rate of 250 °C/min to the preset temperature (T_c) between 30 and 80 °C, and crystallized for three times the peak ending time, to ensure complete crystallization. After isothermal crystallization, the specimens were ready for DSC and WAXD studies. The specimens were scanned up to 140 °C at 10 °C/min to study the melting behavior. The samples were all treated under the same pre-melting conditions, except that the isothermal crystallization time was varied, to study the sequence of occurrence of the multiple melting peaks for the specimens crystallized at 62 °C. They were then scanned directly from T_c up to 130 °C at 10 °C/min.

2.4. Temperature modulated DSC (TMDSC)

Specimens in TA sample pans were prepared isothermally in Pyris 1 DSC under the same conditions as described in DSC section. The TMDSC measurements were made on a TA Instruments Q100 that was equipped with a refrigerating system. The cell constant calibration was performed using an indium standard, and the temperature calibration was conducted using deionized water and indium. A standard sapphire sample was used to measure the heat capacity calibration constant for the modulation study. A heating rate of 2 °C/min with a period of 60 s and a modulation amplitude of 0.20 °C were chosen as a heating-only condition based on the specifications that are presented in the instrument manual [18] and the experiments were evaluated by varying the modulation amplitude, the heating rate, the modulation period and the T_c. To study the effect of the heating rate on the multiple melting peaks, the specimens crystallized at 62 °C were scanned up to 136 °C at 2, 10, 20 and 40 °C/min, respectively, in a conventional mode (DSC).

2.5. Wide-angle X-ray diffraction

Specimens with thickness of about 0.5 mm following completely isothermal crystallization at various T_c values were prepared using Pyris 1 DSC under the same conditions as described in DSC section. X-ray diffractograms at room temperature were obtained using a Siemens D5000 diffractometer with Ni-filtered Cu Kα radiation ($\lambda = 0.1542$ nm, 40 kV, 30 mA) at a scanning rate of 1°/min.

2.6. Polarized light microscopy (PLM)

A Nikon Optiphot-pol polarizing microscope was used in conjunction with a Linkam THMS-600 heating stage and a TMS-91 temperature control system. The video photograph system included a SONY DXC-755 CCD color video camera, a Pioneer DVR-510H DVD recorder and a Linkam VTO-232 video text overlay. Measurements of spherulite growth rates were taken on freshly made film which was made at temperatures between 100 and 105 °C under nitrogen. The specimen was first cooled, then heated at 50 °C/min from room temperature to 140 °C, and kept at 140 °C for 5 min in order to melt the crystalline residues. The pre-molten specimen was cooled down rapidly to the required T_c ranging from 80 to 25 °C. The development of the spherulites was recorded as a function of time during the crystallization process. In each specimen, growth rates were determined for numerous spherulites.

3. Results and discussion

3.1. Wide-angle X-ray diffraction

Fig. 2 presents WAXD patterns of this copolyester following crystallization at various isothermal temperatures. All of the samples yield the same diffraction peaks over the entire range of temperature, indicating only one crystalline form in the samples that were crystallized isothermally between 30 and 80 °C. The crystal unit cell of PES is orthorhombic [7,8], and the diffraction peaks from (120) and (200) planes are observed at $2\theta \approx 20.2°$ and 23.4°, respectively. Based on WAXD patterns, the possibility of different crystal structures is excluded for this study. Therefore, the multiple melting peaks may be due to the melting of different populations of lamellar crystals and/or the melting of recrystallized crystals. The TS comonomer as minor component in the PES-*co*-5%PTS copolymer is in the amorphous state due to the low composition (average-number sequence length of 1.0) and the low melting point of PTS (46 °C) [1].

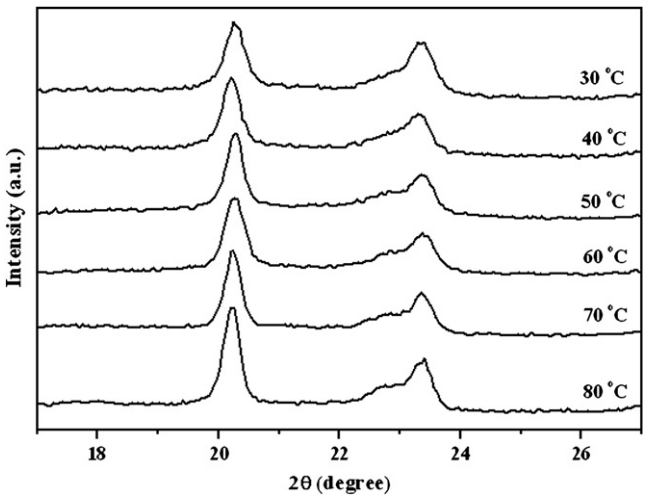

Fig. 2. X-ray diffraction patterns of specimens isothermally crystallized at various temperatures.

3.2. Isothermal crystallization kinetics

Fig. 3 shows DSC exothermic traces for specimens that are isothermally crystallized at temperatures ranging from 30 to 70 °C. DSC traces are not presented for T_c at 75 and 80 °C, because the exothermic heat flow is too slow to be detected during the crystallization process. The second column in Table 1 presents isothermal crystallization time (t_c), at temperatures from 30 to 80 °C. The required t_c declined from 70 min at 30 °C to 40 min at 45 or 50 °C, then increased gradually up to 300 min at 75 °C, finally it was 1000 min at 80 °C. The exothermic trace was integrated to get the heat of crystallization (ΔH_{exo}, column 3), and the absolute crystallinity ($X_{c,exo}$) was calculated by dividing the heat of crystallization by 180 J/g [9]. Column 4 in Table 1 presents the value of $X_{c,exo}$ increases from 22.5% at 30 °C to 27.8% at 65 °C. Owing to the slow isothermal crystallization at $T_c \geq 67$ °C, the values of ΔH_{exo} and $X_{c,exo}$ at 67 and 70 °C were estimated and expressed in parentheses. The values of ΔH_{exo} and $X_{c,exo}$ at 75 and 80 °C were not estimated.

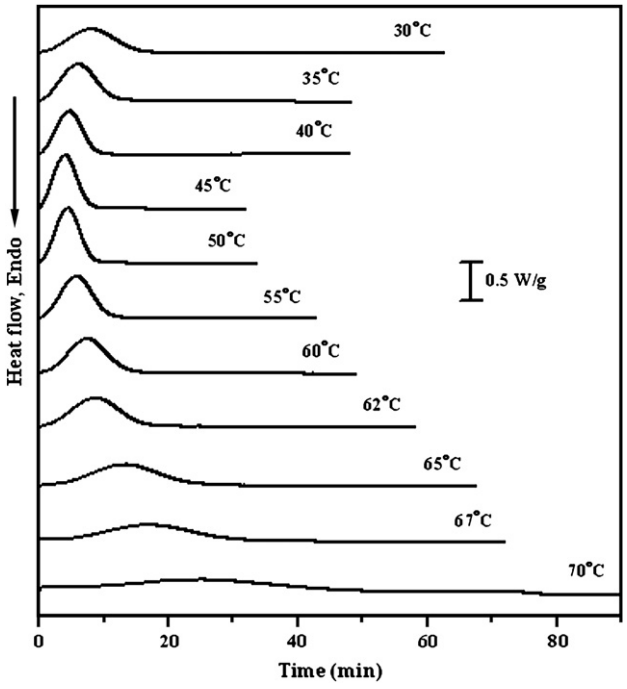

Fig. 3. Crystallization isotherms of specimens at the indicated temperatures (T_c).

The relative degree of crystallinity at time t [$X_c(t)$] was calculated for each T_c. The half-time of crystallization ($t_{1/2}$ – defined as the time required for half of the final crystallinity to develop) was evaluated. The value of $t_{1/2}$ declines from 8.31 min at 30 °C to 3.58 min at 40 °C, then increases gradually up to 19.29 min at 70 °C. The temperature-dependence of the overall crystallization rate ($t_{1/2}^{-1}$) is plotted in Fig. 4 as open squares. It shows a maximum at around 45 °C.

A typical Avrami plot with $\log[-\ln(1 - X_c(t))]$ against $\log t$ is shown in Fig. 5 for the specimen crystallized isothermally at 62 °C. The best linear regression can be made between the relative crystallinities of 2.15 and 99.46% with a correlation coefficient (r^2) of 0.9997, which are tabulated in the row of $T_c = 62$ °C in Table 1. This curve has an initial linear portion corresponding to an Avrami exponent (n_1) of 2.85. A second linear line can be fitted for the leveling off portion. The intersection point of these two linear regression lines was found at 13.83 min, as shown in Fig. 5. The Avrami plots yield n_1 and the rate constant (k_1) at different T_c values. As T_c increases, n_1 increases from 2.70 to 3.16, which are presented in column 7 of Table 1. While k_1 increases first from 2.32×10^{-3} to 1.68×10^{-2}, then declines to 3.91×10^{-4}, which are plotted as filled squares in Fig. 4.

Fig. 4 shows both the maximum values of ($t_{1/2}^{-1}$) and k_1 at 45 °C. The maximum rate of spherulite growth (G) was at 50 °C (described later). Umemoto et al. [11] measured the primary nucleation rate of PES. A maximum was found at 18–32 °C, which depends on the molecular weight. The nucleation rate of PES-*co*-5%PTS is slower than that of PES, because the incorporation of TS units into PES significantly inhibits the crystallization behavior of PES [1]. Therefore, it is expected that the maximum rate of the overall crystallization ($t_{1/2}^{-1}$) is located at a temperature between the temperatures of maximum nucleation rate and maximum growth rate.

The exponent n_1 decreases from 3.16 to 2.70 as T_c decreases. They are less than four, because, first, the thickness of the samples for the DSC studies is around 0.2 mm. At higher T_c values, the nucleation density is low and the

Table 1
Summary of the condition and the kinetic analysis of crystallization for the isothermally melt-crystallized specimens

T_c (°C)	t_c (min)	ΔH_{exo} (J/g)	$X_{c,exo}$ (%, abs)	ΔH_{endo} (J/g)	$X_{c,endo}$ (%, abs)	n_1	$X_c(t)$ range (%, rel)	r^2
30	70	−40.55	22.53	45.90	25.50	2.70	2.59–99.98	0.9997
35	55	−44.08	24.49	47.05	26.14	2.71	4.86–99.95	0.9994
40	55	−44.69	24.83	47.53	26.40	2.73	3.67–99.83	0.9994
45	40	−45.62	25.34	47.82	26.57	2.75	2.61–99.74	0.9994
50	40	−47.66	26.48	50.00	27.78	2.76	2.58–97.79	0.9995
55	50	−48.45	26.92	50.13	27.85	2.81	3.83–96.94	0.9996
60	55	−47.50	26.39	49.85	27.69	2.84	1.14–99.87	0.9998
62	60	−49.90	27.72	50.26	27.92	2.85	2.15–99.46	0.9997
65	80	−50.02	27.79	50.36	27.98	2.92	2.30–98.67	0.9993
67	100	(−45.44)	(25.24)	51.81	28.78	3.16	0.51–99.97	0.9987
70	120	(−37.55)	(20.86)	52.55	29.19	(2.52)	2.00–98.41	0.9993
75	300	–	–	53.23	29.57	–	–	–
80	1000	–	–	55.39	30.77	–	–	–

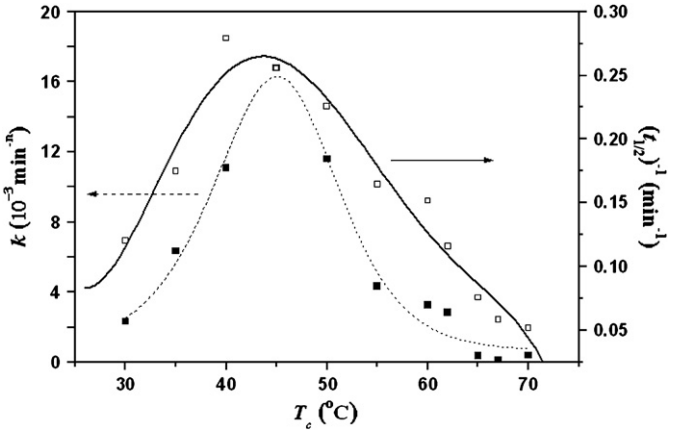

Fig. 4. Temperature dependencies (T_c) of the overall crystallization rate ($t_{1/2}^{-1}$) and the rate constant (k_1).

diameter of the spherulite is about 0.1 mm. Hence, the growth of the spherulites was limited to two dimensions during the later stage of isothermal crystallization. Next, the growth rate of this copolyester is slow with a maximum value of 7.34×10^{-2} μm/s (described later). It is suggested that primary and secondary crystallizations proceeded at the same time before the impingement of crystals (see Table 1 and Section 3.3). Third, the homogeneous nucleation rate increases at lower T_c, representing an athermal nucleation process that is followed by three-dimensional crystal growth in the early stage of isothermal crystallization. Finally, the cooling rate of the refrigerating system is not sufficiently high to avoid crystallization of this copolyester before it was cooled to a lower T_c.

3.3. Elucidating the melting behavior of the specimens crystallized at 62 °C

Some results in the following sections are reported here. The pre-melting condition for the isothermal crystallization was held for 5 min at 160 °C, which is 52 °C higher than T_m^o (108.3 °C, see Fig. 10). Results of thermal stability experiments indicated that PES-*co*-5%PTS was stable in nitrogen up to 200 °C holding for 5 min that will be reported in the next paper. After this pre-melting treatment, the subsequent isothermal crystallization behavior is independent of the prior thermal history. The maximum growth rate of spherulite was 7.34×10^{-2} μm/s at 50 °C. The growth rate was about 6×10^{-2} μm/s at 62 °C. PLM experiments found that the homogeneous nucleation rate of PES-*co*-5%PTS was very slow at temperatures above 60 °C [11,19], and that the regime II → III transition occurred at 65 °C. The crystals formed in regime III usually have more defects and lower crystallinity. These results are used to elucidate the melting behavior following completely isothermal crystallization at 62 °C.

Fig. 6 presents DSC thermograms at a heating rate of 10 °C/min for specimens that have been isothermally crystallized at 62 °C. Enlarged thermograms at around 67 °C are inserted in the left side of this figure. Specimens crystallized isothermally for 4 or ≥8 min, yield double or triple melting peaks, respectively. The peak temperatures of the melting peaks are denoted T_{m1}, T_{m2} and T_{m3} in the order of increasing temperature (same in Figs. 7 and 9). Small amount of exothermic phenomenon can be found between the two upper melting peaks, and the amount of exotherm increases slightly with the crystallization time. However, this exothermic curve is relatively small comparing with the peak at T_{m3}, because both the nucleation rate and the growth rate are slow (or the recrystallization rate is slow) at 62 °C. Therefore, the ratio of intensities of the peak at T_{m3} and that at T_{m2} varies very little. These results indicate that the upper peaks at T_{m2} and T_{m3} appear first and the lower peak at T_{m1} occurs after further crystallization. The minimum time for the occurrence of T_{m1} (∼8 min) is shorter than 13.83 min (see Fig. 5). As shown in the last three columns of Table 1, the relative crystallinity range (up to ∼99%) for the initial linear portion also suggests that the endothermic peak at T_{m1} (the secondary process) takes place before the spherulites have impinged on each other.

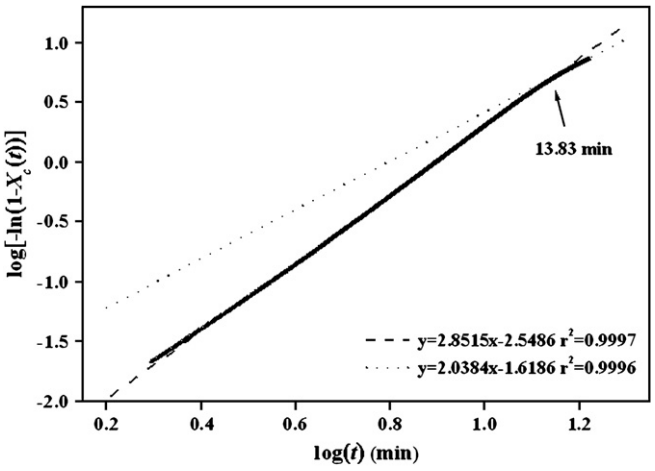

Fig. 5. Plot of $\log[-\ln(1 - X_c(t))]$ vs. $\log t$ for specimens crystallized isothermally at 62 °C.

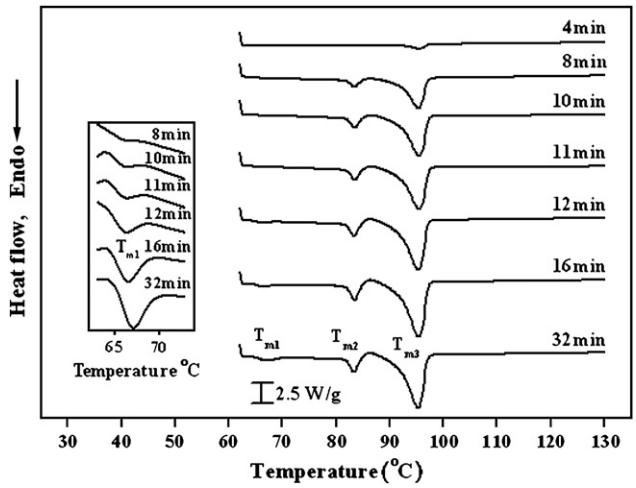

Fig. 6. DSC thermograms (at a heating rate of 10 °C/min) for specimens after pre-melting at 160 °C for 5 min and then crystallized isothermally at 62 °C for various periods of time.

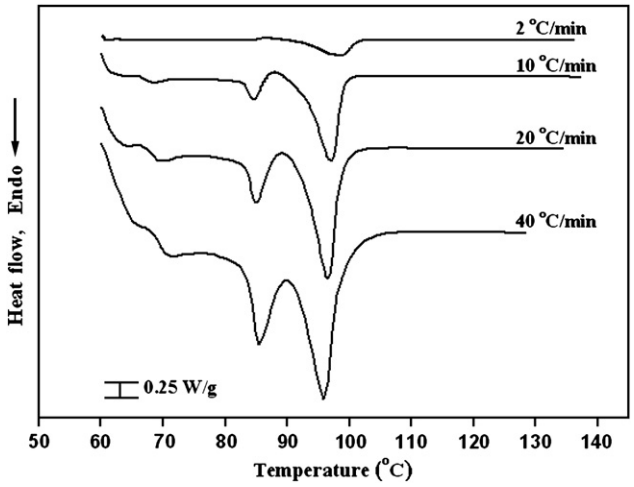

Fig. 7. DSC thermograms at different heating rates for specimens crystallized isothermally at 62 °C. These measurements were made on a TMDSC instrument in a conventional mode.

Fig. 7 shows conventional DSC thermograms at four different heating rates for specimens after complete isothermal crystallization at 62 °C. When the heating rate increases from 2, 10, 20 to 40 °C/min, triple melting peaks can be observed and described as follows. The peaks at T_{m1} (~69 °C) and T_{m2} (~85 °C) shift to higher temperature and increase in intensity. The exothermic peak just prior to the major melting peak (T_{m3}) gradually decreases to zero. The peak at T_{m3} (~97 °C) shifts to lower temperature and even its intensity increases with increasing the heating rate. The ratio of intensities of the upper two melting peaks decreases significantly as the heating rate increases because less time is available for the recrystallization and/or reorganization during the heating scan.

Fig. 8 shows the TMDSC curves at a heating rate of 2 °C/min for the specimen isothermally crystallized at 62 °C. In the total curve (symbol as T), a small exothermic peak at around 86 °C can be detected just prior to the melting of the main peak. TMDSC cannot discriminate quantitatively among reversible (symbol as R) and non-reversible (abbreviated as NR) contributions of polymer melting [20–22]. Only qualitative approach is described below. In the NR and total curves, the exothermic enthalpy constitutes direct evidence of the melting–recrystallization–remelting of PES-*co*-5%PTS copolyester. However, the main melting peak in the total curve is contributed mainly from the reversible melting at a heating rate of 2 °C/min. At a higher heating rate, 10 °C/min in Fig. 7, the recrystallization exotherm becomes less, i.e. the contribution of the remelting to the main melting peak becomes less. The remelting peak is distinct in the case of PES with a viscosity molecular weight of 10,000 [12,13]. The molecular weight of PES [24] synthesized in this lab is higher than that of any PES used in the cited papers [2,9,12–14]. It can be found that the maximum growth rate presented in cited paper of Ref. [24] is only half of that shown in cited paper of Ref. [2]. As mentioned in Section 1 [1], the incorporation of TS units into PES significantly inhibits the crystallization behavior of PES. The growth rate and recrystallization rate of this PES-*co*-5%PTS are expected to be slower than those of PES. Therefore the peaks at T_{m2} and T_{m3} in Figs. 6–8 are primarily due to the melting of different populations of lamellar crystals.

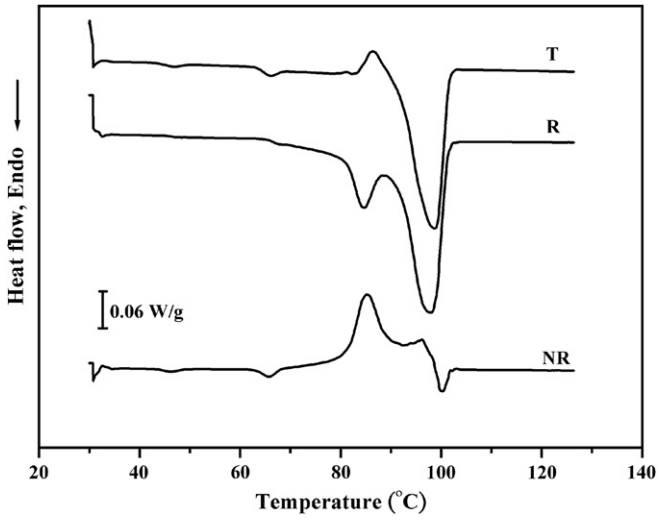

Fig. 8. TMDSC thermograms at a heating rate of 2 °C/min with a period of 60 s and a modulation amplitude of 0.20 °C for specimens crystallized isothermally at 62 °C.

3.4. Elucidating the melting behavior using conventional DSC

Fig. 9 displays the results of DSC heating scans at a heating rate of 10 °C/min. The heating curves show multiple endothermic peaks. A small exothermic peak can be detected just before the melting of peak at T_{m3}, and is denoted as T_{exo}. T_{m1} is about 5–10 °C above T_c. The peak at T_{m2} appears when $T_c \geq 60$ °C and becomes a major peak for $T_c \geq 75$ °C. The peaks at T_{m1} and T_{m2} shift to higher temperature and increase in intensity as T_c increases. This trend reveals that thicker crystalline lamellae develop as T_c increases. The position and intensity of the peak at T_{m3} vary very slightly with T_c, but the integrated area of this peak declines as T_c increases

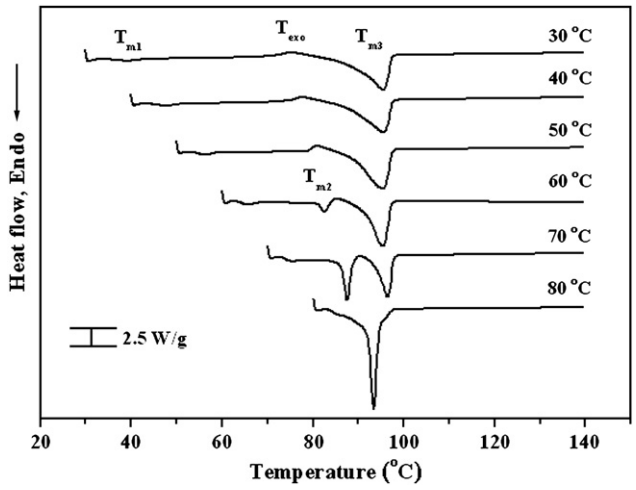

Fig. 9. DSC thermograms (at a heating rate of 10 °C/min) for specimens isothermally melt-crystallized at the indicated temperatures.

from 30 to 70 °C. The ratio of intensities of the peak at T_{m3} and that at T_{m2} increases significantly as T_c decreases, because the melting temperature of the secondary crystals (T_{m1}) decreases, and more time is allowed to recrystallize during the heating scan. These results reveal that lower temperature part of the peak at T_{m3} is related to the melting of the recrystallized crystals. As T_c increases, the contribution of melting–recrystallization–remelting process to the upper melting peak gradually decreased and finally disappeared. Therefore, the peak at T_{m2} is attributed to the fusion of the crystals grown during primary crystallization and the peak at T_{m1} is associated with the secondary crystals. In addition, melting temperature can be rigorously defined as the melting of the last trace of crystals and is denoted as $T_{m3\text{-end}}$. The numerical value of $T_{m3\text{-end}}$ remains constant at 98.1 ± 0.2 °C. The total enthalpy of melting (ΔH_{endo}) is measured and listed in the fifth column of Table 1. Its value increases from 45.9 to 55.4 J/g as T_c increased from 30 to 80 °C. The corresponded absolute crystallinity ($X_{c,endo}$) increases from 25.5 to 30.8%, as shown in the sixth column of Table 1.

Fig. 10 shows T_{m1} and T_{m2} as a function of T_c. A solid line is drawn where $T_m = T_c$. The values of T_{m1} (open squares) fall on a line with a slope of 0.892, becoming close to the $T_m = T_c$ line as T_c increases. According to the Hoffman–Weeks approach [23], the values of T_{m2} are extrapolated (based on the linear regression of the open circle points with T_cs = 60, 62, 65, 67, 70, 75 and 80 °C) until they intersect with the solid line. The temperature of the intersection is T_m^o, with a value of 108.3 °C. This value is about 10 °C higher than $T_{m3\text{-end}}$. This T_m^o estimated from the Hoffman–Weeks plot may be less reliable, but the regime transition temperature $T_{II \to III}$ can be assumed to be almost independent of the values of T_m^o [24].

3.5. Kinetic analysis of the growth rates of spherulites

The growth rate (G) of spherulites was determined before their impingement by measuring the spherulitic radii from PLM micrographs taken at successive intervals during the isothermal crystallization. Fig. 11 plots the temperature-dependence of the growth rate as open triangle. The growth rate increases smoothly from 1.17×10^{-2} μm/s at 25 °C, passes a maximum of 7.34×10^{-2} μm/s at 50 °C, then decreases smoothly to 0.51×10^{-2} μm/s at 80 °C. The growth rates of PES [19,25] are also plotted in Fig. 11 as open squares. The maximum growth rate of this PES-*co*-5%PTS copolyester is about half of PES. One of the reasons is that the incorporation of TS units into PES significantly inhibits the crystallization behavior of PES [1].

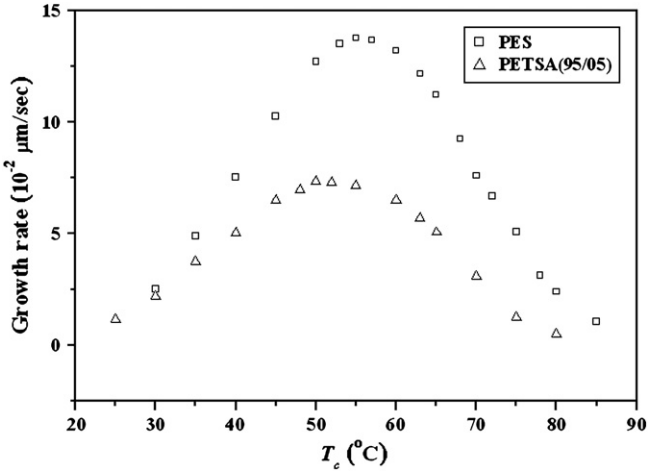

Fig. 11. Variation of spherulitic growth rates with temperature.

The regime analysis based on the LH model [17] is used to treat the growth rate data presented in Fig. 11. Fig. 12 plots $\log G + U^*/[2.303R(T_c - T_\infty)]$ as a function of $1/(T_c \Delta T f)$ yielding the value of K_g (slope × 2.303) in each regime. R represents gas constant. U^* and T_∞ denote the WLF (Williams–Landel–Ferry) energy term and WLF temperature, respectively, $\Delta T = (T_m^o - T_c)$ is the undercooling, and f represents a correction term of the order of unity, which is usually given by

$$f = 2T_c/(T_m^o + T_c) \quad (1)$$

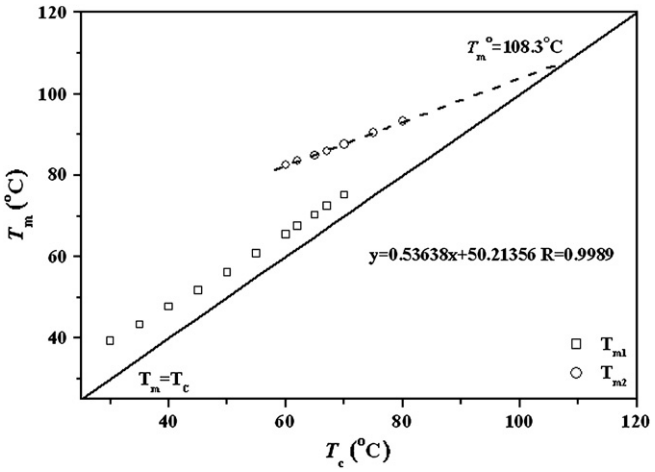

Fig. 10. Hoffman–Weeks plot for determining the equilibrium melting temperature of the copolyester from conventional DSC data at a heating rate of 10 °C/min.

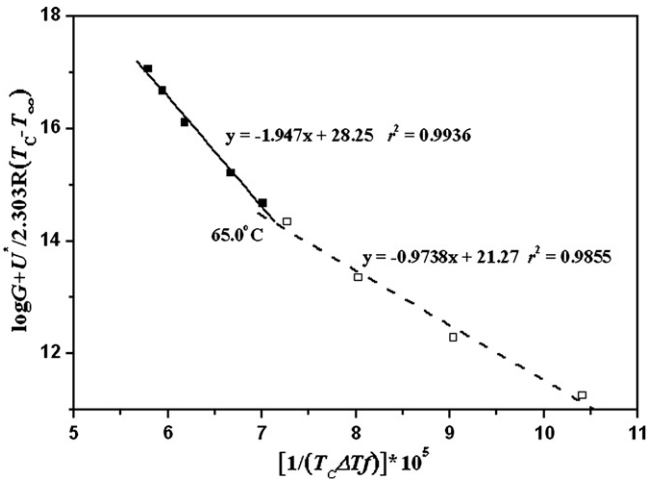

Fig. 12. Kinetic analysis of the growth rate data of spherulites. In this case, $U^* = 11{,}500$ cal/mol, and $T_\infty = T_g - 51.6$ K.

Table 2
Values of K_g, correlation coefficient and transition temperature determined from secondary nucleation theory

T_∞ (K)	U^* (cal/mol)	K_g(III) $\times 10^{-5}$	r^2(III)	K_g(II) $\times 10^{-5}$	r^2(II)	K_g(III)/K_g(II)	$T_{II\rightarrow III}$ (°C)
T_g-30	1500	–	–	–	–	–	–
T_g-30	7000	4.085	0.9929	2.037	0.9856	2.00	64.6
$T_g-51.6$	4200	1.767	0.9969	1.303	0.9914	1.36	64.4
$T_g-51.6$	11,500	4.484	0.9936	2.243	0.9855	2.00	65.0

The regime analysis of the LH model was performed by using the following values: $U^* = 11{,}500$ cal/mol, and $T_\infty = T_g - 51.6$ K with T_g at 261.5 K. $T_m^o = 108.3\,^\circ\text{C} = 381.4$ K was adopted. The two optimal fit lines correspond to the correlation coefficients (0.994 and 0.986), as shown in Fig. 12. The curve is broken at $T_c = 65.0\,^\circ\text{C}$ and the ratio of the two slopes is 2.00, which are tabulated in the fourth row of Table 2.

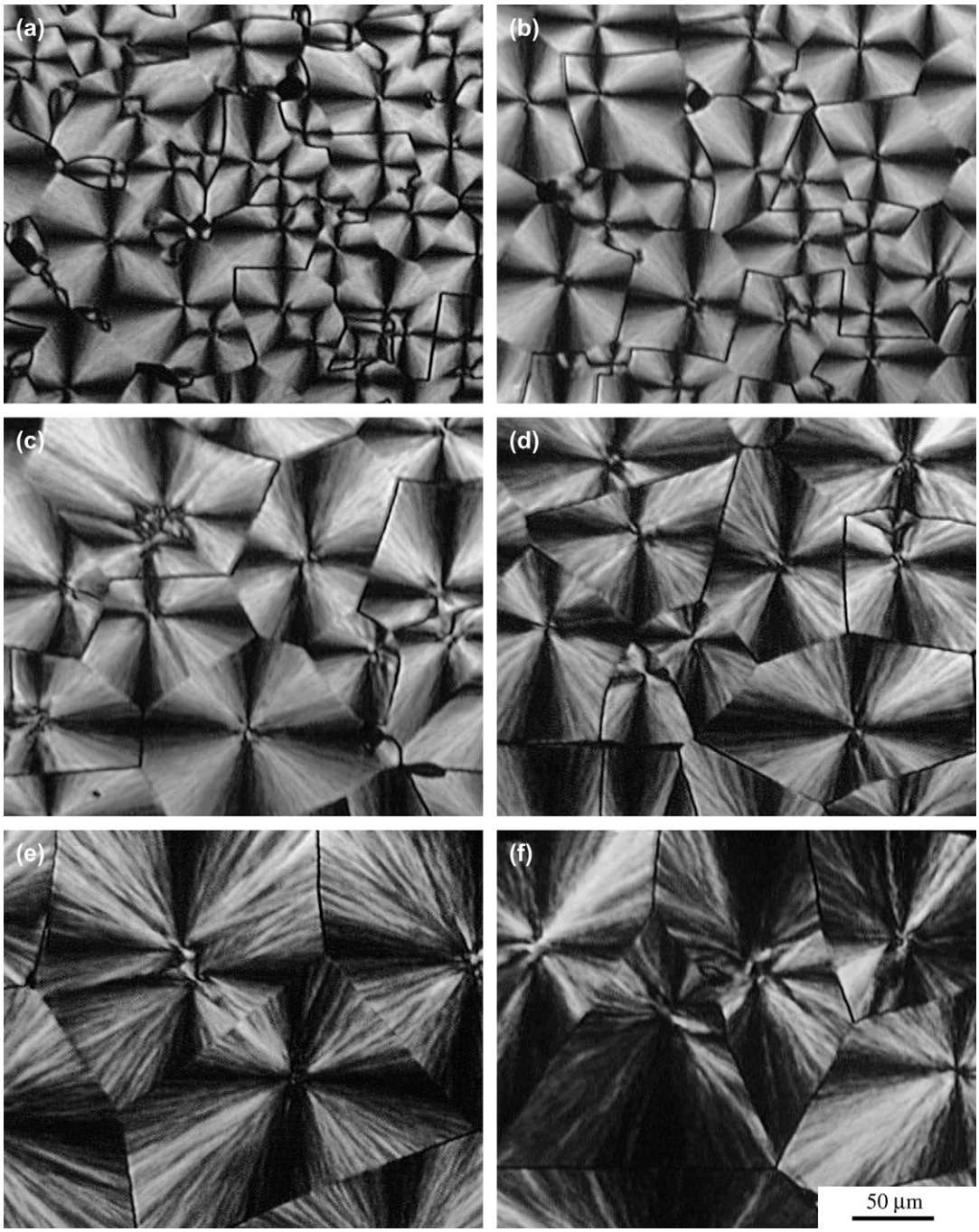

Fig. 13. Representative PLM micrographs for specimens melt-crystallized at the indicated temperatures: (a) 50, (b) 55, (c) 61, (d) 63, (e) 65, and (f) 70 °C.

In Table 2, the variation of T_∞ and U^* was tried, and the calculated values of K_g, correlation coefficient (r^2), $T_{II\to III}$ are listed between columns 4 and 9. In the first and second rows where T_∞ is $T_g - 30$ K, $T_{II\to III}$ is not found when U^* is 1500 cal/mol, the ratio of $K_g(III)/K_g(II)$ is 2.00 when U^* is 7000 cal/mol. The value of $T_{II\to III}$ is 64.6 °C. In the case of $T_\infty = T_g - 51.6$ K and $U^* = 4200$ cal/mol, the ratio of $K_g(III)/K_g(II)$ is 1.36 and the value of $T_{II\to III}$ is 64.4 °C (see row 3). These results reveal that PES-*co*-5%PTS exhibits a regime II → III transition at 64.7 ± 0.2 °C which is about 6 °C less than that of PES [19,25].

Fig. 13 presents the samples, crystallized from the melt at various T_c, between the crossed polaroids. The optical behavior of these spherulites exhibited typical negative birefringence, marked with a dark Maltese cross. There was no abrupt change in morphology when T_c was increased from 25 to 61 °C. Gan et al. [2] demonstrated that the radiating lines from the center of the PES spherulites became coarse with the increase in T_c. They examined the morphological changes at spherulitic level and lamellar level in regimes II and III by using a PLM and atomic force microscope, and indicated that there was indeed a transition from regime II to regime III at around 71 °C. Similarly, the increase in the coarseness of the PES-*co*-5%PTS spherulites can be assumed from 63 to 70 °C, as shown in the textures of Fig. 13, parts d–f.

4. Conclusion

This PES-*co*-5%PTS copolyester is found to have 94.4 mol% ethylene succinate (ES) units and 5.6 mol% trimethylene succinate (TS) units. The value of the random parameter, 1.06, is close to 1.0 for a random copolymer. The average-number sequence lengths of ES and TS units are 16.8 and 1.0, respectively. A single T_g also suggests that this copolymer is a random copolyester. Isothermal crystallization indicated that the n_1 values of the Avrami exponent decreased from 3.2 to 2.7 as T_c decreased from 67 to 30 °C. At higher T_c, the n_1 values of the Avrami exponent are less than the theoretical value of 4 because the secondary crystals might already grow within the primary crystal lamellae. The maximum rate of the overall crystallization is expected to be located at a temperature (45 °C) between the temperature of maximum nucleation rate and the temperature of maximum growth rate (50 °C). The growth rate data are examined with the Hoffman–Lauritzen nucleation theory. The classical regime II → III transition occurs at around 65 °C.

WAXD patterns suggest that there is only one crystal structure formed isothermally between 30 and 80 °C. Conventional DSC and TMDSC curves revealed triple melting peaks. The melting behavior showed that the upper two melting peaks appear first and then the lower melting peak occurs at a longer crystallization time. A small exothermic behavior between the upper two melting peaks provides direct evidence of recrystallization. As T_c increases, the contribution of recrystallization gradually decreases and finally disappears. The absence of exothermic flow and the appearance of triple melting peaks support the mechanism that involves various lamellar crystals. The Hoffman–Weeks linear plot gave an equilibrium melting temperature of 108.3 °C which is 10.2 °C higher than the melting temperature of the last trace of crystals.

Acknowledgements

The authors acknowledge the financial support of the National Science Council of Taiwan, ROC, through Grant NSC 94–2216–E-110-020.

Appendix. Supplementary data

Supplementary data associated with this article can be found, in the online version, at doi:10.1016/j.polymer.2007.06.060.

References

[1] Tsai CJ, Chang WC, Chen CH, Lu HY, Chen M. Eur Polym J, under revision.
[2] Gan Z, Abe H, Doi Y. Biomacromolecules 2000;1:704.
[3] Kumagai Y, Kanesawa Y, Doi Y. Makromol Chem 1992;193:53.
[4] Bikiaris DN, Papageorgiou GZ, Achilias DS. Polym Degrad Stab 2006;91:31.
[5] Fuller CS, Erickson CL. J Am Chem Soc 1937;59:344.
[6] Bunn CW. Proc R Soc London 1942;A180:67.
[7] Ueda AS, Chatani Y, Tadokoro H. Polym J 1971;2:387.
[8] Ichikawa Y, Washiyama J, Moteki Y, Noguchi K, Okuyama K. Polym J 1995;27:1264.
[9] Papageorgiou GZ, Bikiaris DN. Polymer 2005;46:12081.
[10] Takayangi M. J Polym Sci 1955;19:200.
[11] Umemoto S, Hayashi R, Kawano R, Kikutani T, Okui N. J Macromol Sci Phys 2003;B42:421.
[12] Al-Raheil IA, Qudah AMA. Polym Int 1995;37:249.
[13] Caminiti R, Isopo A, Orru MA, Albertini VR. Chem Mater 2000;12:369.
[14] Qiu ZB, Komura M, Ikehara T, Nishi T. Polymer 2003;44:7781.
[15] Avrami M. J Chem Phys 1939;8:212.
[16] Avrami M. J Chem Phys 1941;9:177.
[17] Hoffman JD, Davis GT, Lauritzen Jr JI. In: Hannay NB, editor. Treatise on solid state chemistry, vol. 3. New York: Plenum Press; 1976 [chapter 7].
[18] TA Instruments. DSC 2910 differential scanning calorimeter, Operator's manual, Rev. 8. New Castle, Delaware; 1997. p. C-73.
[19] Chang WC. Master thesis, National Sun Yat-sen University, Kaohsiung, Taiwan; 2006.
[20] Wurm A, Schick C. Colloid Polym Sci 2003;281:113.
[21] Di Lorenzo ML, Wunderlich B. Thermochim Acta 2003;405:255.
[22] Wunderlich B. Prog Polym Sci 2003;28:383.
[23] Hoffman JD, Weeks JJ. J Res Natl Bur Stand 1962;66A:13.
[24] Gan Z, Abe H, Kurokawa H, Doi Y. Biomacromolecules 2001;2:605.
[25] Lu HY, Peng JS, Chen M, Chang WC, Chen CH, Tsai CJ. Eur Polym J 2007;43:2630.